



Modeling and mapping the spatiotemporal variation in agricultural drought based on a satellite-derived vegetation health index across the highlands of Ethiopia

Zerihun Chere^{1,3} · Assefa Abegaz¹ · Lulseged Tamene² · Wuletawu Abera²

Received: 21 February 2022 / Accepted: 3 June 2022 / Published online: 30 June 2022
© The Author(s), under exclusive licence to Springer Nature Switzerland AG 2022

Abstract

Drought is the most complex, devastating, slow-onset natural disaster and has recently affected more people than ever before. Remote sensing has recently played a vital role in providing huge amounts of data for monitoring and modeling the incidence of droughts at broad spatiotemporal scales. Therefore, the objective of the current study in Ethiopia's highlands was to model and map the spatiotemporal patterns, status, and trends of agricultural drought based on the satellite-derived vegetation health index (VHI) on a monthly (June–September) scale from 2004 to 2018. The study used Terra Moderate Resolution Imaging Spectroradiometer (MODIS) Land Surface Temperature and Emissivity 8-Day (MOD11A2) and Enhanced Moderate Resolution Imaging Spectroradiometer Normalized Difference Vegetation Index (eMODIS NDVI) datasets. During data analysis, the VHI, Mann–(MK) Kendall's trend test, and Sen's slope estimator were used, respectively, to grade agricultural drought, investigate agricultural drought trends, and examine the magnitude of agricultural drought change. Crop yield data for 41 crop growing zones was used to evaluate the capability of VHI for agricultural drought monitoring. The results showed the VHI detected moderate to severe agricultural droughts. Seasonally, 26.3% of the total crop growing areas showed a decreasing VHI trend. In most northern, central, and southeastern Ethiopia, the correlation analyses between VHI and crop yields showed good relationships. The findings of the current study display the importance of mapping the spatiotemporal patterns of agricultural droughts using VHI, aiming at agricultural drought monitoring and establishing early warning and decision-making systems.

Keywords Agricultural drought · Vegetation condition index · Temperature condition index · Vegetation health index

Abbreviations

VHI	Vegetation health index
LST	Land surface temperature
NDVI	Normalized difference vegetation index
TCI	Temperature condition index
VCI	Vegetation condition index

Introduction

Declared as a naturally occurring, slow onset, and most complex disaster, droughts are an extended incidence of an abnormally dry period and inadequate rainfall to satisfy usual requirements, resulting in massive damage to human beings, agriculture, and livestock (Mishra and Singh 2010; Mutsotso et al. 2018; Mishra et al. 2022; Patil et al. 2021). Drought can occur anywhere in the world regardless of the region's normal precipitation rates and trends (Mishra and Singh 2010; Hayes et al. 2011; Bhaga et al. 2020), and its onset and end are difficult to detect and highly unpredictable (Bhaga et al. 2020). In terms of the number of people affected globally, it is the first natural hazard (Baniya et al. 2019). Drought has a vast range of consequences that influence many different sectors of society (Mishra and Singh 2010; Kogan et al. 2019). However, its immediate impact is highly related to crop production and farm employment by reducing soil water availability and increasing pest infections

✉ Zerihun Chere
zerihunchere@gmail.com

¹ Department of Geography and Environmental Studies, Addis Ababa University, P.O. Box 150375, Addis Ababa, Ethiopia

² Alliance for Bioversity International and Center for Tropical Agriculture (CIAT), Addis Ababa, Ethiopia

³ Department of Geography and Environmental Studies, Dire Dawa University, Dire Dawa, Ethiopia

(Sai et al. 2016), which leads to considerable losses in crop failure and pasture losses and creates food insecurity (Kogan et al. 2019; Bayable and Gashaw 2021). Apart from its huge impact on a large number of people living on Earth, drought has been a very costly disaster in countries of Africa and Asia (Bayissa et al. 2018; Kogan et al. 2019; Qu et al. 2019).

More than 85% of the Ethiopian population's economy is mainly dependent on rain-fed agriculture, which is sensitive to climate change (Bayissa et al. 2018; Liou and Muluaem 2019). Droughts that affected the majority of the country were documented in the years 1983–1984, 1994–1995, 2009–2010, and 2014–2015 (Viste et al. 2013; Degefu and Bewket 2015; Liou and Muluaem 2019). Overall, 2015 was identified as the driest year, with 10.2 million people affected (Liou and Muluaem 2019; Qu et al. 2019). In Ethiopia's highlands, specifically in the northern and central highlands, where the study area is located, agricultural drought is currently more pronounced (Gebrehiwot et al. 2016).

Drought indices are used to detect and monitor agricultural drought and hence provide a valuable means of scientifically evaluating the magnitude and impact of droughts and offering policy recommendations (Mishra and Singh, 2010; Ihinegbu and Ogunwumi 2021). Since agricultural drought results from complex and nonlinear interactions between climate, soil systems, crop phenology, and socioeconomic activities, monitoring its frequency/intensity, spatial variability, and impact has continued to be a challenging task for drought managers and policymakers (Sai et al. 2016). As a result, developing regionally and locally fitted early agricultural drought management and analysis mechanisms that can serve as an integral part of the nation's efforts to prevent drought-related losses is critical.

Precipitation indices, remote sensing data (Wilhite 2011), and agricultural sample surveys have been used to explore and monitor agricultural droughts. Agricultural sample surveys are traditional, time-consuming, and expensive. In addition, stand meteorological indices, such as the standardized precipitation index (SPI), rainfall anomaly index (RAI), Palmer drought severity index (PDSI), and standardized precipitation-evapotranspiration index (SPEI), have been commonly used to monitor drought in various regions aimed at characterizing agricultural droughts (Mishra and Singh 2010; Vicente-serrano et al. 2010; Nam et al. 2015; Rahman and Lateh, 2016; Miah et al. 2017; Yisehak and Zenebe 2020; Haile et al. 2022). However, both agricultural surveys and alone stand precipitation index approaches did not produce continuous spatial data to monitor the detailed drought conditions (Gu et al. 2007; Gidey et al. 2018). Various remote sensing indices, such as the normalized difference vegetation index (NDVI) (Tucker 1979; Anyamba and Tucker 2012), vegetation condition index (VCI), temperature condition index (TCI), and vegetation health index (VHI) (Kogan 1995; Karnieli et al. 2006) have been used for

agricultural drought monitoring to overcome this shortcoming over the last decades. According to Bhuiyan et al. (2017) and Gidey et al. (2018), remote sensing-based agricultural drought monitoring gives more accurate, adaptable, and dependable results in drought studies (Bhuiyan et al. 2017; Gidey et al. 2018).

Previous studies on the monitoring of agricultural droughts in Ethiopia were based on SPI (Edossa et al. 2010; Viste et al. 2013; Degefu and Bewket 2015; Mohammed et al. 2018), combined SPI and VCI (Gebrehiwot et al. 2011) and VCI (Gebrehiwot et al. 2016). Despite a large number of remote sensing-based studies on agricultural and vegetation-related drought in Ethiopia, there are still uncertainties and major gaps to be considered. For example, the studies mentioned above (1) mainly relied on NDVI data derived from a coarse spatial resolution from mixed spatial coverage of agricultural and nonagricultural areas, (2) did not exclusively focus on annual crop growth periods/seasons, and (3) did not consider temperature conditions (LST), while recently, due to global warming, the role of temperature in drought monitoring has become crucial. Evaluating the spatiotemporal dynamics of agricultural drought by incorporating climatic elements (LST) is important for policymakers to establish effective and comprehensive monitoring and early warning systems to reduce the negative effects of drought.

Thus, in this study, agricultural drought monitoring was conducted on a four-month time scale (i.e., June–September) with VHI and Mann–Kendall (MK) nonparametric rank-based trend analysis by exclusively focusing on annual agricultural croplands. The stated time-scale is the main annual rain-fed crop growing period of the highlands of Ethiopia. Therefore, studying agricultural drought during this time-scale with VHI that combines VCI of moisture and TCI relying on the thermal infrared (TIR) (Singh et al. 2003; Bhuiyan et al. 2006) can provide better information. Therefore, this is the first study of its kind to look at agricultural drought through VHI and MK nonparametric rank-based long-term agricultural drought monitoring in Ethiopia in general and in the highlands of Ethiopia in particular. The objectives of this study were to (1) explore the spatiotemporal dynamics of agricultural drought and (2) examine the frequency of agricultural drought in the highlands of Ethiopia from 2004 to 2018.

Materials and methods

The study area

The study covers the highlands of Ethiopia, which lie above 1500 m above sea level; situated between 3° 48' 5" N and 14° 37' 28" N and 34° 12' 6" E and 42° 58' 48" E (Fig. 1), and it occupies an area of 320,442 square

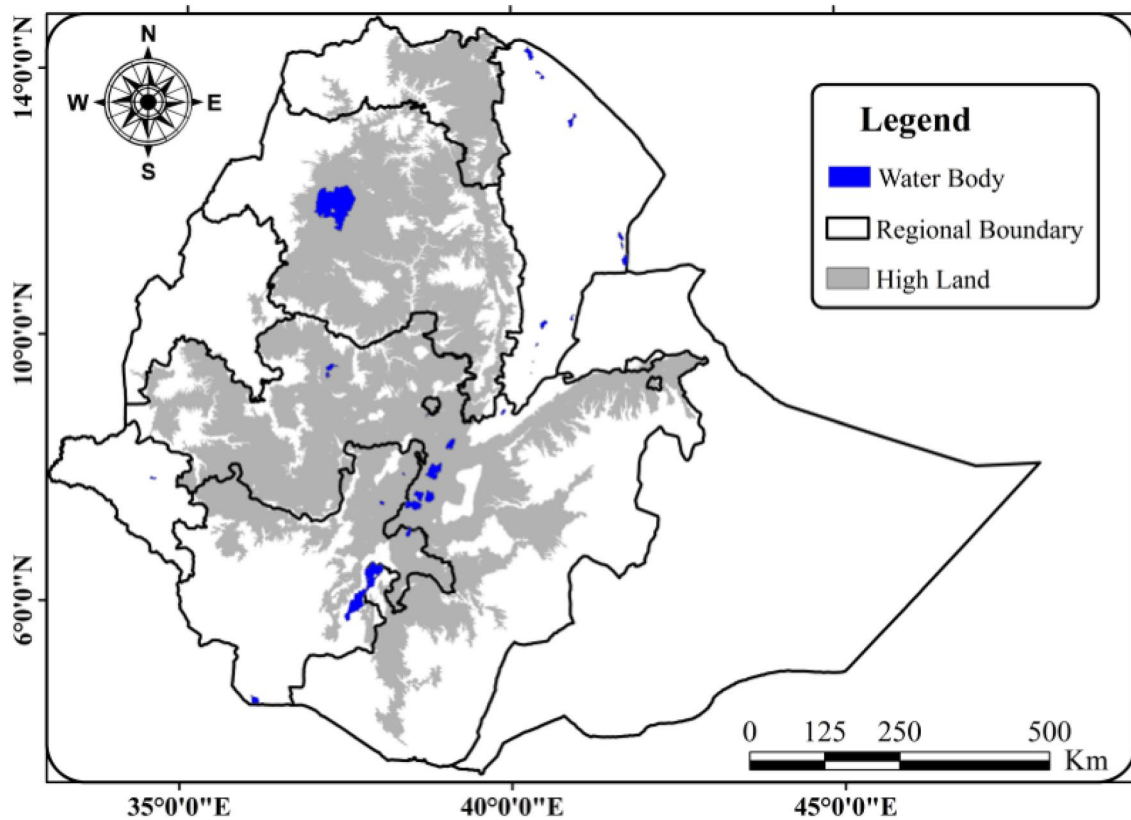


Fig. 1 Location map of the study area (extracted from CSA 2007; GADM 2018)

kilometers. The climatic zone is defined as a humid subtropical highland (Beyene and Meissner 2010) with a regional annual average rainfall of ~ 1100 mm (Dinku et al. 2018). The general rainfall pattern is monomodal (Kiremt and long rain season) (June–September), with short rainy seasons (March–May).

The total annual rainfall (65–95%) in the region is contributed by the long rainy season accounts (Segele and Lamb 2005). Nearly 90–95% of the annual food crops of Ethiopia are being grown during the Kiremt season in the region. The mean annual minimum and maximum temperatures are 7.9 °C and 21.1 °C, respectively (Dinku et al. 2018). The highlands of Ethiopia are home to over 90% of Ethiopia’s population, as well as approximately 90% of the country’s cultivated land and 60% of the country’s livestock (Hurni et al. 2010). Small-scale and subsistence mixed agriculture is practiced by Ethiopian farmers in the highlands.

Data acquisition

In this study, NDVI, LST, and land use land cover (LULC) (area of the cropland of the highlands of Ethiopia) were used as input data.

Terra eMODIS NDVI

In this study, we obtained multitemporal smoothed decadal enhanced moderate imaging spectrometer (eMODIS) normalized difference vegetation index (NDVI) raw data for the East Africa window from the Famine Early Warning System Network (FEWS-NET) from 2004 to 2018 (June–September) with a 250 m spatial resolution. We used Terra eMODIS-NDVI data because, for agricultural drought monitoring, it is said to be superior to Aqua eMODIS data and data of other satellite images, such as SPOT-Vegetation (Swets 1999; Gidey et al. 2018; Jenkerson et al. 2010). The monthly eMODIS-Terra NDVI data were calculated and used as an input to calculate the VCI and VHI, as part of an integrated agricultural drought monitoring approach.

Land surface temperature (LST)

In addition to NDVI, LST has been used as a criterion for examining the situation of vegetation health since the Earth’s surface temperature affects vegetation growth (Kogan 1995; Frey and Kuenzer 2015; Gidey et al. 2018). The ultimate reason for selecting these data is the better spatial, temporal variation, and up-to-date algorithm (Frey et al. 2012). The eight-day MOD11A2 Terra LST

data with a 1-km spatial resolution were downloaded from <https://lpdaacsvc.cr.usgs.gov/appeears/> for the 4 months of the Ethiopian crop growing period. The monthly LST of each month was calculated using the 8-day LST and used as an input to calculate the TCI and VHI.

Furthermore, the anomaly hot spots of agricultural production (ASAP) dataset on cropland and rangeland masks was used for agricultural areas (Fig. 2). These data were mainly obtained by evaluating eight global datasets through a multicriteria analysis (MCA) (Pérez-Hoyos et al. 2017).

In this study, only cropland information is used to extract the NDVI, LST, TCI, and VCI statistics for the detection of agricultural droughts. Cereal crops (teff, wheat, and maize) at the administrative zonal scale (shown in Fig. 2) were used to evaluate the VHI. The crop yield data were obtained from Ethiopia's Central Statistical Agency (CSA). The crop yield data collected for the Kiremt season represent 90–95% of Ethiopia's annual total crop production. Crop yield data for 41 administrative zones were thus collected for the period 2004 to 2018. However, 3 years of data (2009, 2017, and 2018) were missing and therefore discarded.

Data processing and analysis

Identification of drought

The spatiotemporal variation in agricultural drought from 2004 to 2018 (15 years) was characterized using drought grades defined by the VHI. The VHI can detect and describe the duration, spatial distribution, frequency, and/or status of agricultural drought (Bhuiyan et al. 2006; Choi et al. 2013; Kogan and Guo 2016; Ma'rufah et al. 2017; Patil et al. 2021). The VHI monitors overall vegetation health by combining the vegetation condition index and the temperature condition index during a certain period (Kogan and Guo 2016; Kogan 2019).

Vegetation condition index (VCI) The VCI is a means of quantifying the relative healthiness of vegetation in response to weather (Kogan 1995). According to Singh et al. (2003), the VCI can indicate the cumulative environmental influence on vegetation. It rescales the dynamics vegetation between 0 (bad) and 100 (optimal) (Kogan 2019). Before computing the VCI, 10-day composite eMODIS NDVI raw data for the study area were masked out and rescaled between -1 and 1 using the ArcGIS 10.5.1 package as follows (Eq. 1):

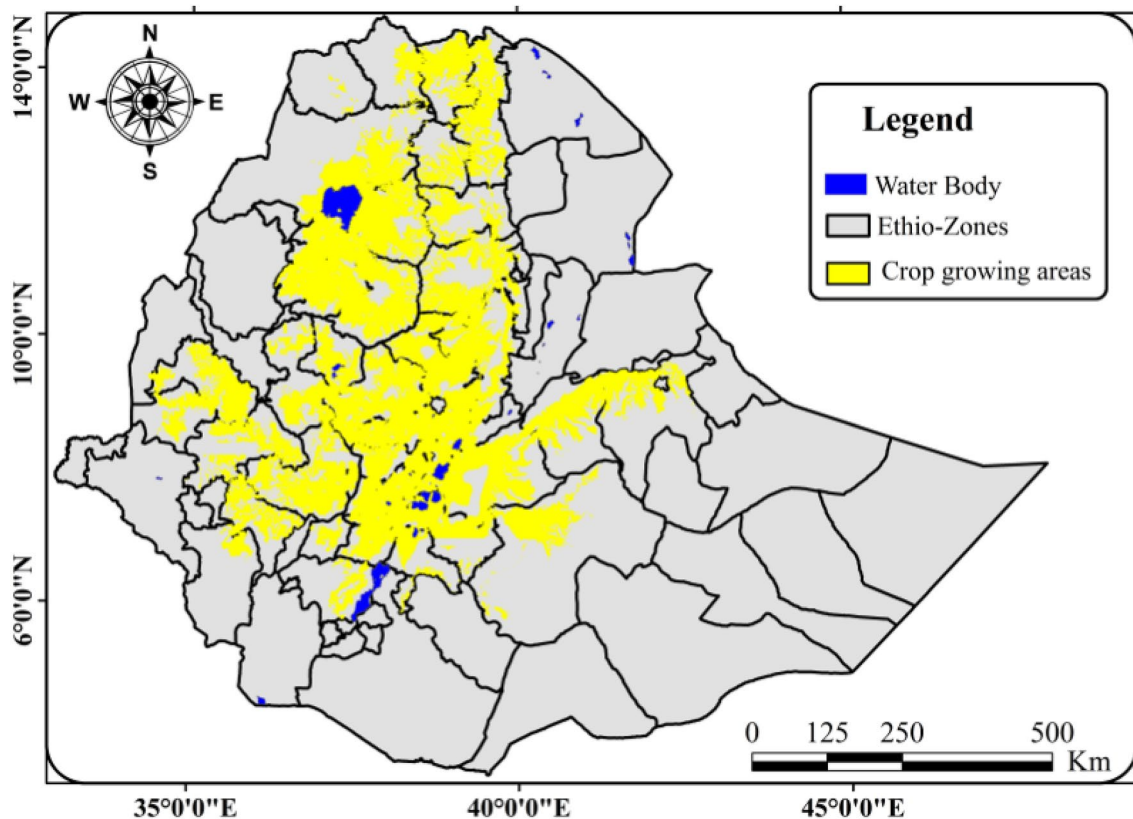


Fig. 2 The spatial locations of the crop growing area (GADM 2018; ASAP/EU 2019 crop mask)

$$eMODISNDVI = \text{Float}(\text{SmoothedeMODISNDVI} - 100)/100. \tag{1}$$

Then, the VCI was derived as (Eq. 2) based on Kogan (1995).

$$VCI = 100 \times (NDVI_i - NDVI_{min}) / (NDVI_{max} - NDVI_{min}), \tag{2}$$

where $NDVI_i$ is the current smoothed NDVI value of the i th month, whereas $NDVI_{min}$ and $NDVI_{max}$ are a multiyear (2004–2018) absolute minimum and maximum NDVI value for every pixel at a particular period, respectively.

Temperature condition index (TCI) Currently, because of global warming, the role of temperature in drought monitoring is crucial, and only using the NDVI-based VCI index is not sufficient to fully characterize agricultural drought (Hasan and Mahmud-ul-islam 2015).

In this study, the four MOD11A2 Terra 8-day LST data were added and divided by four in a raster calculator to obtain the mean monthly LST, which was then resampled to 250 m to correspond to the eMODIS NDVI data. The valid LST value was rescaled and converted into degree Celsius ($^{\circ}C$) units (Wan 2006) as follows (Eq. 3):

$$LST = (\varpi \times 0.02) - 273.15, \tag{3}$$

where ϖ = row scientific data (RSD).

As a thermal stress indicator, the TCI incorporates temperature-related drought scenarios (Kogan 2019). Thus, it is important to use the TCI to identify temperature-induced vegetative stress for drought monitoring (Karnieli et al. 2010). TCI was utilized to capture various responses of vegetation to in situ temperature (Cai et al. 2018; Zeng et al. 2022) and computed as (Eq. 4) based on Kogan (1995).

$$TCI = 100 \times (LST_{max} - LST_i) / (LST_{max} - LST_{min}), \tag{4}$$

where LST_i is the LST value of the i th month (June–September), whereas LST_{max} and LST_{min} are the smoothed multiyear maximum and minimum LSTs (2004–2018, 15-year records), respectively. Similar to the VCI, the TCI varies from 0 (a water stress condition) to 100 (an optimal moisture condition).

Vegetation health index (VHI) Finally, the VHI that represents the overall health of the vegetation and is used to identify drought (Karnieli et al. 2006; Zeng et al. 2022) is computed by combining the TCI and the VCI (Eq. 5) as proposed by Kogan (1995, 2019).

$$VHI = a \times VCI + (1 - a) \times TCI, \tag{5}$$

where ‘ a ’ is a coefficient determining the contribution of TCI and VCI and is generally taken as 0.5. Drought conditions are defined as extreme drought, ≤ 15 ; severe drought, 16–25;

moderate drought, 26–40; and no drought (no effect on agriculture) > 40 , according to a recent study by Kogan (2019).

In addition, the frequency of agricultural drought was determined by calculating the mean value of VHI for administrative zones during the Kiremt season (June–September) from 2004 to 2018. Consequently, all observations below the mentioned threshold (40%) were counted for each month (June, July, August, and September) for 15 years (overall 60 months).

Agricultural drought trend detection

The Mann–Kendall (MK) method is a nonparametric test method that does not require a normally distributed data series (Mann 1945), is widely used to identify a monotonic trend in the time series of the vegetation condition index (Baniya et al. 2019) and climate by using remote sensing and hydrometeorological data (Zeng et al. 2022) and is a nonparametric test method that does not require a normally distributed data series. We used the MK trend test to detect the spatial and temporal patterns of VHI changes pixel by pixel using monthly (June–September) datasets (2004–2018). The Mann–Kendall test compares the slopes of all pairs of samples to detect a monotonic trend (Katila et al. 2020). The MK statistics S for time series data (Y_t , $t = 1, 2, \dots, n$) are calculated according to Pohlert (2020) as (Eq. 6):

$$S = \sum_{j < i}^n \text{Sig}(Y_i - Y_j), \tag{6}$$

where Y_i and Y_j are the monthly mean VHI values in years i and j , respectively, $i > j$, and n is the length of the time series data. The sign of all possible differences $Y_i - Y_j$ is computed as follows (Eq. 7):

$$S(Y_i - Y_j) = \begin{cases} +1, & \text{if } Y_i - Y_j > 0 \\ 0, & \text{if } Y_i - Y_j = 0 \\ -1, & \text{if } Y_i - Y_j < 0 \end{cases} \tag{7}$$

When $n \geq 8$, the statistic S is approximately normally distributed with mean $E[S] = 0$ and variance σ^2 given by the following equation (Eq. 8):

$$\sigma^2 = \left\{ n(n-1)(2n+5) \sum_{j=1}^p t_j(t_j-1)(2t_j+5) \right\} / 18, \tag{8}$$

where p and t_j are the number of tied groups in the time series dataset and the number of data points in the j th tied group, respectively.

Then, the test statistic Z is calculated as follows (Eq. 9):

$$\begin{cases} \frac{S-1}{\sigma}, & \text{if } S > 1 \\ 0, & \text{if } S = 0 \\ \frac{S+1}{\sigma}, & \text{if } S < 1 \end{cases} \quad (9)$$

The null hypothesis (H_0) states that there is no trend in the series, whereas the alternative hypothesis (H_1) states that the series has an increasing or decreasing monotonic trend. The magnitude of the linear trend was then predicted following Sen's slope estimation procedure (Sen 1968; Li et al. 2017). The change per unit time of a trend was computed as follows (Eq. 10):

$$\text{Sen's slope} = \text{Median}\{(X_i - X_j)/(i - j)\}, i > j, \quad (10)$$

where X_i and X_j are the changing monthly VHI values at times i and j , respectively. There is not significant variation over time, with a value near zero. As an average change, the slope of the monthly VHI trend is computed. A negative value shows a downward trend, and a positive value shows a positive trend. The positive (upward) VHI slope values indicate increased vegetation growth as a consequence of no-or reduced drought, while the negative (downward) trends specify a decrease in vegetation cover as a result of rising drought (Qian et al. 2016). The trend analysis for VHI was performed using TerrSet software (Neeti and Eastman 2011).

Evaluating the VHI prediction capability of agricultural drought in the highlands of Ethiopia

Because agricultural yields and productivity are impacted by several factors, including scientific and technical breakthroughs (e.g., improvements in plant genetics and fertilizer) as well as weather and climatic conditions, assessing drought losses over time and space is challenging (Lu et al. 2017). We concentrated on the influence of climate on crop yield rather than other factors in this study. Thus, in this study, detrending (simple linear regression model), which removes the upward linear trend of crop yields (Wu et al. 2007; Lu et al. 2017), was used. Twelve years of crop yield data were used to detrend the zonal yield statistics as (Eq. 11):

$$Y_{dt} = Y_{at} - (Y(t) = \beta X(t)), \quad (11)$$

where Y_{dt} is the detrended yield at time t ; Y_{at} is the actual yield at time t ; $Y(t)$ is the predicted yield at time t , α is the y -intercept (the estimated value of the crop yield at time $t=0$ or first-year record), β is the slope of the trend line (or the average change in crop yield per year), and $X(t)$ is the year that the yield is estimated.

Finally, the capabilities of the VHI for agricultural drought monitoring in the highlands of Ethiopia were evaluated using a simple linear regression model. The annual

cereal crop production was correlated with the September VHI time series. September was chosen because the vegetation cover (NDVI) in most parts of Ethiopia's highlands had achieved its maximum value (Gebrehiwot et al. 2011; Bayissa et al. 2018). Simple linear regression and Pearson correlation can provide either positive or negative results. This ranges between 0 and +1 (Table 1). Regression or Pearson correlation values close to zero indicate no relationship between the indices.

The Evans standard (1996) was adopted to determine the level of the Pearson correlation matrix and coefficient of determination (R^2) strengths (Table 1, Fig. 3).

Results and discussions

Validation of the VHI prediction capability of agricultural drought

The spatial and temporal relationships between the detrended crop yield and VHI (at the end month of the Kiremt rainfall season, September) for the 41 selected crop growing zones were investigated. Figure 4 shows the spatial correlation determination values between the vegetation health index (VHI) and detrended maize crop yield in the crop growing areas. The regression analysis results showed that the relationship between the VHI and maize crops in 34 out of 35 crop growing zones was positive, moderate ($R^2/r=0.16/0.40$ to $R^2/r=0.35/0.59$) to strong ($R^2/r=0.3.6/0.60$), and statistically significant in 14 crop growing zones ($P < 0.05$). A strong correlation was observed in the West Harerge, Wag Himra, Oromia, Eastern Tigray, East Harerge, North Gondar, East Gojjam, North Shewa3, Asosa, Keffa, and Jimma zones, while a moderate correlation was observed in all zones of the South Nations, Nationalities and Peoples (SNNP) of Ethiopia.

Regarding teff, the northern and central highlands of Ethiopia showed a strong correlation with the rest of the study area. A high regression result (R^2) between teff and VHI was observed in the Southern Tigray Zone ($R^2=0.56/r=0.75$ or; $P < 0.01$). Likewise, in 10 zones, the regression value was $r > 0.5$ or $R^2=0.25$, and 8 of these values were statistically significant ($P < 0.05$). Furthermore, the correlation between

Table 1 Strengths of Pearson bivariate correlation coefficients and linear regression model (Source: Evans 1996)

Level of statistical strength	Pearson correlation matrix (r)	Coefficient of determination (R^2)
Strong	$\geq 0.60, \leq -0.60$	≥ 0.36
Moderate	$0.40-0.59, -0.40$ to (-0.59)	$0.16-0.35$
Weak	-0.40 to 0.40	< 0.16

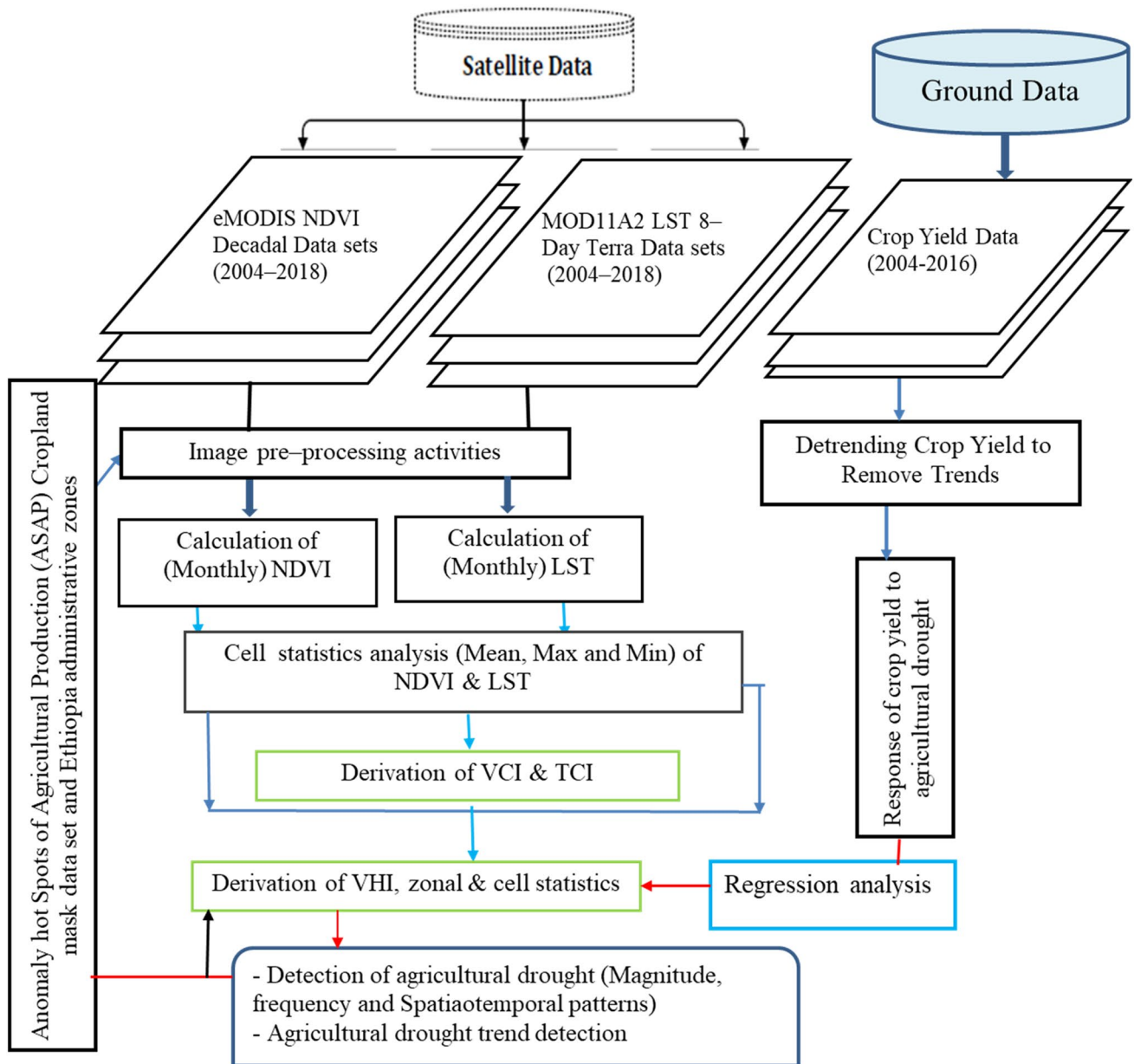


Fig. 3 Methodological flow chart for modeling the incidence of agricultural drought

wheat yield and VHI in the 9 zones was statistically significant at $P < 0.05$. Similarly, Kogan et al. (2018) observed a solid relationship between wheat yield and VHI in Australia during the crop growing period. Generally, a higher relationship between VHI and crop yield was observed in the northern, central, southeastern, and some zones in the southern and southwestern parts of Ethiopia. The spatial correlation pattern obtained in this study is consistent with the pattern noted in Tadesse et al. (2015) and Bayissa et al. (2018), who attempted to evaluate evapotranspiration products and CDI-E with cereal crop yield, respectively. Typically, the evaluations presented here advise that VHI is suitable for

agricultural drought monitoring in the highlands of Ethiopian agricultural management systems.

Modeling the spatial and temporal agricultural drought patterns based on VHI

The spatiotemporal pixel-based VHI investigation over the Kiremt season from 2004 to 2018 in the highlands of Ethiopia showed a wide range of drought conditions (moderate to extreme) during the crop growing periods of 2004, 2005, 2009, 2010, 2014, and 2015 in the central, northern and southeastern highlands of Ethiopia, where the land is mainly

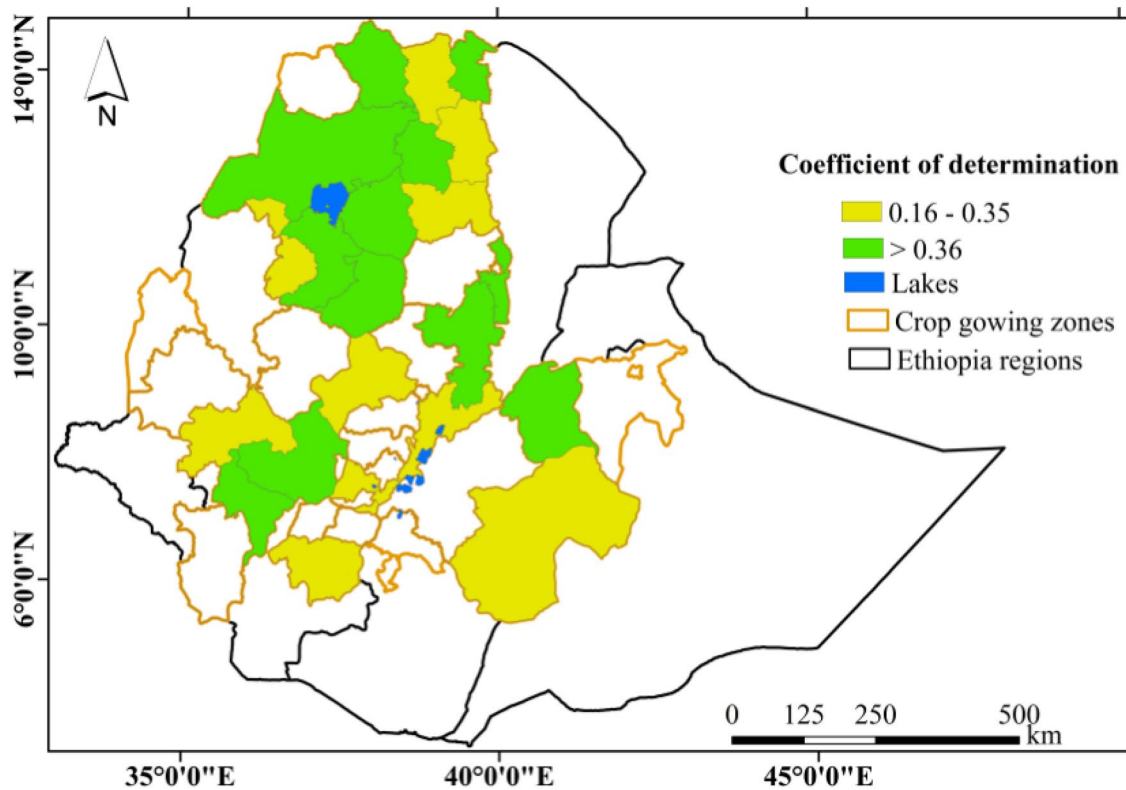


Fig. 4 Spatial distribution of correlations between the vegetation health index (VHI) and detrended maize crop yield in the crop growing areas

covered by rain-fed agriculture. According to Liou and Muluaem (2019), the 2009–2010 and 2014–2015 droughts in Ethiopia were the direct influence of ENSO. In contrast, the years 2006, 2007, 2008, 2011, 2012, 2013, 2016, 2017, and 2018 exhibit near-normal vegetation conditions, which could indicate a good crop harvest. This study's findings matched those of Liou and Muluaem (2019), who documented severe drought years in Ethiopia's central, northern, and eastern parts during the Kiremt season in 2002–2004, 2009–2010, and 2014–2015. In addition, Bayable and Gashaw (2021) reported drought years in the upper part of the Awash basin in 2002–2003, 2009–2010, and 2012–2014.

Figure 5 depicts spatiotemporal VHI patterns during the Kiremt season for selected extensive drought years (2004, 2009, 2010, 2014, and 2015) as well as a wet year (2018). A large portion of the study area was affected by severe drought in 2009 and 2015. By studying the VHI map of 2009 from June to September, drought conditions were prevalent in most parts of the study area, ranging from moderate to extreme. It was found that 30–78% of the total area was affected by moderate to extreme drought conditions (Fig. 6). For instance, in June 2009, 78% of the total area was under drought, of which 42% was under extreme drought conditions. Likewise, in July 2009, 45% of the study area was under drought, with 6% of the area under extreme drought

conditions. In August and September of 2009, the total area affected by extreme drought was 5% and 11%, respectively. During August, the total area affected by drought was reduced, probably because of the heavy precipitation during August 2009 over the western and northern highlands of Ethiopia (Bayissa et al. 2018). In 2009, a severe drought affected the central, northern, and northwestern parts of the study area.

Similarly, the portion of the area affected by agricultural drought during the 2015 cropping season ranged from 40 to 48% (Fig. 6). In June, it was revealed that 43% of the study area was under drought conditions, with 3%, 16%, and 24% areas under extreme, severe, and moderate drought conditions, respectively.

The total areas affected by extreme drought in July and August were 6% and 8%, respectively. In 2015, the central, southeastern, and northern parts of the study area experienced extreme drought conditions. On the other hand, in June, July, and August 2018, more than 85% of the study area showed normal conditions. However, due to the failure of rainfall, moderate to extreme drought conditions in September affected a relatively large portion of the study area (22%) (Fig. 6).

The findings of this study aligned with those of Viste et al. (2013), who stated that 2009 was the only year during

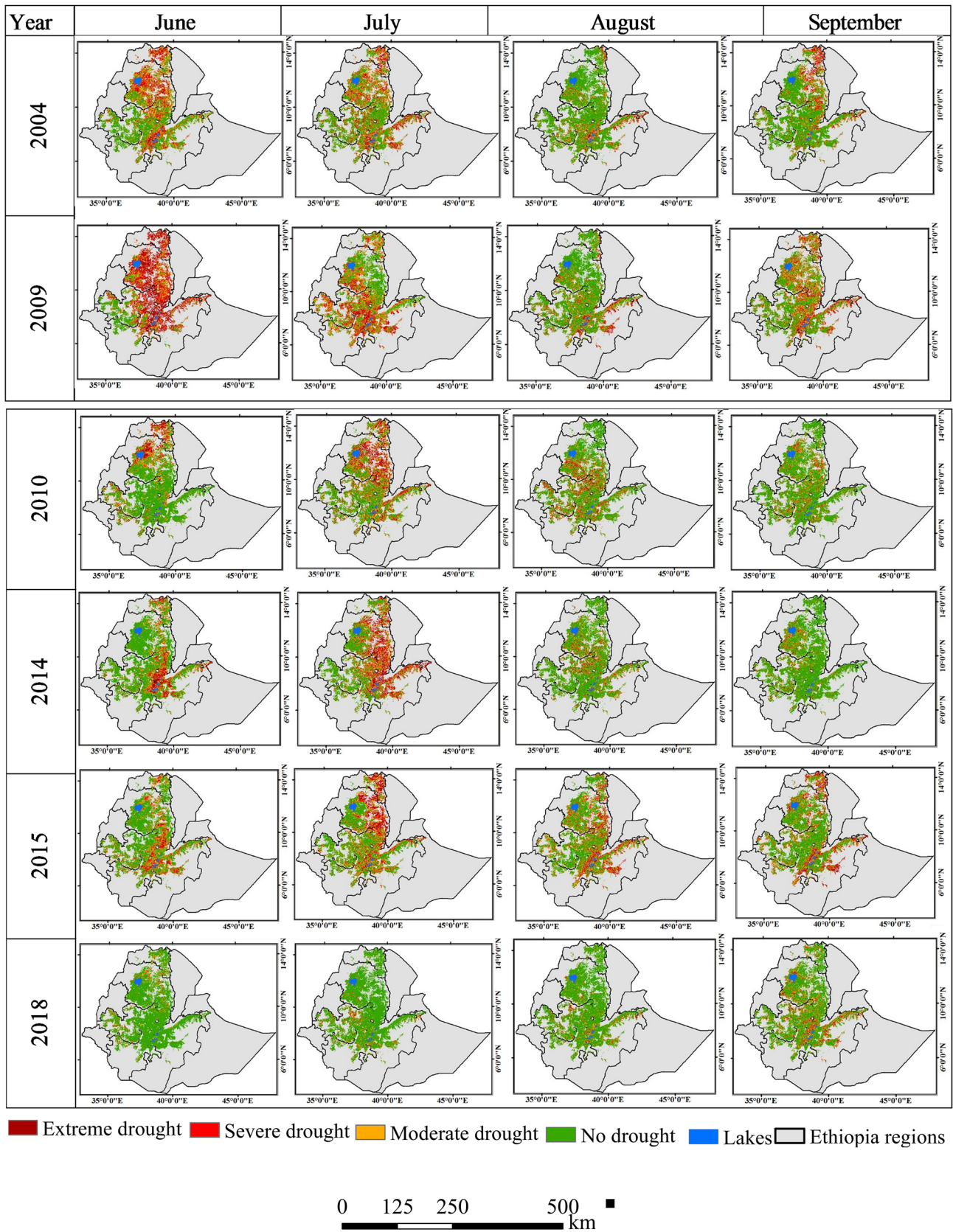


Fig. 5 Spatial pattern of agricultural drought in the highlands of Ethiopia using the vegetation health index (VHI) for drought years (2004, 2009, 2010, 2014, and 2015) and normal years (2018)

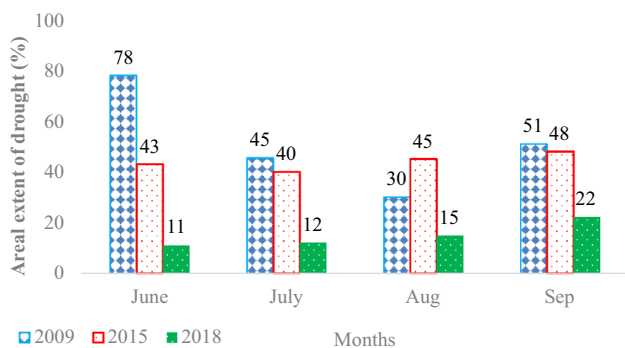


Fig. 6 The area affected (%) by moderate to extreme drought conditions for drought years (2009 and 2015) and normal years (2018)

1972–2011 that most zones of Ethiopia were struck by moderate to severe drought conditions, and Sohnesen (2020) and Qu et al. (2019), who reported that 2015 was a drought year with low rainfall in the growing season.

Status and frequency of agricultural droughts

Table 2 depicts the frequency of agricultural droughts in Ethiopia’s highlands. The northern and southeastern highlands had the highest frequency of agricultural drought, while the southern and southwestern highlands had a lower incidence of agricultural drought, with the area experiencing nearly 1–4 drought occurrences (Table 2).

Table 2 Frequency of agricultural drought incidence per administrative zones at a monthly time scale from 2004 to 2018

Zones	E	S	M	T	Zones	E	S	M	T
Asosa			2	2	East Harargie		3	8	11
Awı		1	3	4	East Shewa	2		14	16
South Gonder	1	2	10	13	North Shewa4	1		8	9
South Wollo		4	8	12	Alaba	1	4	10	15
West Gojjam		2	8	10	Benchi Maji			2	2
East Gojjam	1	1	6	8	Gamo Gofa			6	6
North Shewa3		3	7	10	Gedeo			4	4
Oromia	2	3	8	13	Gurage		1	3	4
North Gonder		2	10	12	Hadiya			4	4
North Wollo		5	7	12	Keffa			1	1
Wag Himra		5	9	14	Kembata Tembaro			4	4
Arsi	1		6	7	Sidama		2	6	8
Bale			12	12	Silti		1	12	13
South West Shewa	1		9	10	Wolayita		1	6	7
East Welega			4	4	Yem			6	6
Illubabor			3	3	Southern Tigray		1	13	14
Jimma			4	4	Central Tigray	1	1	16	18
West Welega			3	3	Western Tigray		2	10	12
West Harare	1	2	9	12	Eastern Tigray	1	2	14	17
West Shewa	1		5	6	North Western Tigray	1	3	8	12

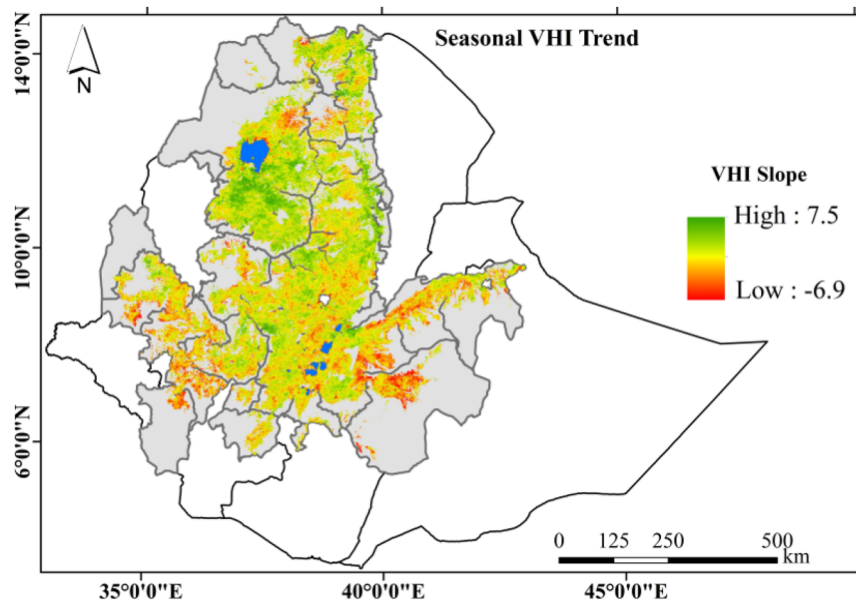
E extreme drought, S severe drought, M moderate drought, T total periods in which drought occurred

During the study period, the northern and central highlands (Tigray and Amhara regions), Ormia’s East and West Hararge, East Shewa Zones, and Southern Nations Nationalities and people’s Alaba, Sidama, and Silti zones were delineated as drought-prone zones. These findings are supported by the findings of Gebrehiwot et al. (2016).

Spatial and temporal drought (VHI) trends

The spatial and temporal VHI trends of Ethiopia’s highlands in the Kiremt season varied geographically from – 6.9 to 7.5 from 2004 to 2018 (Fig. 7). A negative trend was observed in 26.3% of the crop growing areas, with only approximately 3.6% being statistically significant at $p < 0.05$. Negative VHI slope values were observed in the study area’s southern, southwestern, and northern parts, which indicates a potential drought-vulnerable area due to reduction and fluctuation in rainfall. On the other hand, the VHI discovered a positive trend in 73.6% of crop-growing areas, with just 13% of those statistically significant. The areas with no changes in VHI make up a small portion of the total (0.01%).

Regarding the monthly VHI trend, the southeastern, southwestern, and central parts of the study area experienced a decreasing pattern in June (Fig. 8). In this month, the VHI slope values varied from – 8.7 to 7.7, and 20.5% of the study area showed a downward trend, with 2.7% being statistically significant at $P < 0.05$. However, the majority of the study area (79.3%) showed a positive pattern, with only 0.2%



■ No agricultural land use □ Ethiopia boundary ■ Lakes ■ Zone boundary

Fig. 7 Spatial patterns of seasonal VHI slope in the highlands of Ethiopia (2004–2018)

of areas showing no change in VHI. During July, the VHI trend showed a declining pattern with slope values ranging from -6.3 to 6.8 , and 47.9% of the study area showed a decreasing pattern, out of which 2.1% was statistically significant. All studied zones in Tigray, Amhara (North Wollo, Waghimra, North Gondar, South Wollo, and North Shewa), Oromia (East Shewa, Bale, and North Shewa), and SNNP (Hadiya and Wolayita) experienced a decreasing VHI trend.

During August, 45.1% of the pixels had a diminishing VHI pattern. In this month, however, 52% and 2.9% of pixels, respectively, indicated an increasing and no change trend. Furthermore, during September, the VHI slope values ranged from -21.2 to 24.1 , with 36% of the study area showing a downward trend. Furthermore, only 5.1% of pixels showed a statistically significant declining pattern, and the results are similar to those of Liou and Muluaem (2019).

Conclusion

This study employed VHI and MK nonparametric rank-based trend analysis to investigate the spatiotemporal variation in agricultural drought throughout the growing season in Ethiopia’s highlands for 15 years, from 2004 to 2018. Droughts of moderate to extreme severity were recorded by

the VHI in 2004, 2005, 2009, 2010, 2014, and 2015. However, the years 2006, 2007, 2008, 2011, 2012, 2013, 2017, 2016, and 2018 showed near-normal VHI in the majority of the studied areas. The years 2009 and 2015 were found to be major drought years. Spatially, the most vulnerable agricultural production areas were identified as the central and northern highlands (especially the Amhara and Tigray regions), East Shewa4, East and West Harargie, Silti, and Alaba zones. Pixel-based trend analysis showed that a significant VHI decreased significantly in the southeastern, southwestern, and northern parts of the area of study. Furthermore, the regression analysis between VHI and detrended maize showed a stronger positive correlation than teff and wheat. A strong positive relationship between maize and VHI was observed in the West Harargie zone ($R^2/r = 58.8/76.7$; $P < 0.01$). In southern Tigray, on the other hand, there was a substantial connection between VHI and teff ($R^2 = 0.56/r = 0.75$; $P < 0.01$) and ($R^2 = 0.45/r = 0.67$; $P < 0.05$). Overall, a higher relationship between VHI and detrended crop yields was observed in the northern and central highlands of Ethiopia. As a result, the findings from this study will be used by planners and policymakers to create effective and comprehensive monitoring and early warning systems to minimize and lessen the severe effects of drought in drought-affected areas of the highlands of Ethiopia.

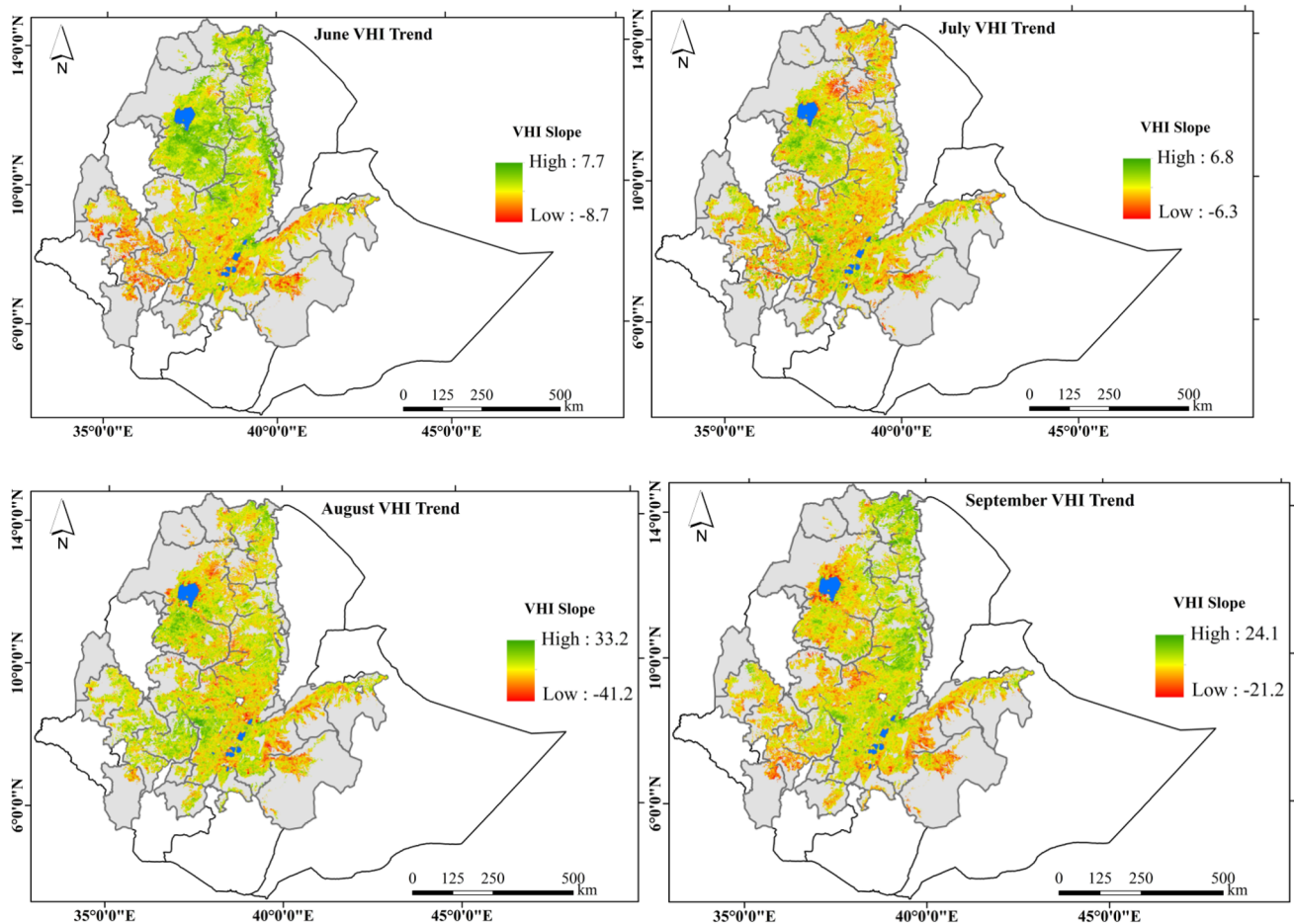


Fig. 8 Monthly (June–September) spatial pattern of VHI slope in the highlands of Ethiopia (2004–2018)

Acknowledgements This research was undertaken with financial support from the Federal Ministry of Economic Cooperation and Development (Bundesministerium für wirtschaftliche Zusammenarbeit und Entwicklung, BMZ).

Author contributions ZC initiates the research topic, conducts a literature review, designs scientific techniques, collects data, analyzes it, and interprets it, prepares draft manuscripts for publication. AA, LT, and WA provide feedback on the research idea, provide advice on the overall research activities, and improve the manuscript. All of the authors provided their in-depth knowledge of the study. The final manuscript was read and approved by all authors.

Data availability statement The datasets generated and analyzed during the current study are available from the corresponding author on reasonable request.

Declarations

Conflict of interest The authors declare that they have no known competing financial interests or personal relationships that could have appeared to influence the work reported in this paper.

References

- Anyamba A, Tucker CJ (2012) Historical perspectives on AVHRR NDVI and vegetation drought monitoring. *Remote Sens Drought Innov Monit Approaches*. <https://doi.org/10.1201/b11863>
- Baniya B, Tang Q, Xu X, Haile GG, Chhipi-Shrestha G (2019) Spatial and temporal variation of drought based on satellite-derived vegetation condition index in Nepal from 1982–2015. *Sensors* 19(2):430. <https://doi.org/10.3390/s19020430>
- Bayable G, Gashaw T (2021) Spatiotemporal variability of agricultural drought and its association with climatic variables in the Upper Awash Basin, Ethiopia. *SN Appl Sci* 3(4):1–20. <https://doi.org/10.1007/s42452-021-04471-1>
- Bayissa YA, Tadesse T, Svoboda M, Wardlow B, Swigart J, Van Andel SJ (2018) Developing a satellite-based combined drought indicator to monitor agricultural drought: a case study for Ethiopia developing a satellite-based combined drought indicator to monitor agricultural drought: a case study for Ethiopia. *Giosci Remote Sens* 00(00):1–31. <https://doi.org/10.1080/15481603.2018.1552508>
- Beyene EG, Meissner B (2010) Spatio-temporal analyses of correlation between NOAA satellite RFE and weather stations' rainfall

- record in Ethiopia. *Int J Appl Earth Obs Geoinf* 12:S69–S75. <https://doi.org/10.1016/j.jag.2009.09.006>
- Bhaga TD, DubeT SMD, Shoko C (2020) Impacts of climate variability and drought on surface water resources in sub-saharan africa using remote sensing: a review. *Remote Sens* 12(24):4184
- Bhuiyan C, Singh RP, Kogan FN (2006) Monitoring drought dynamics in the Aravalli region (India) using different indices based on ground and remote sensing data. *Int J Appl Earth Obs Geoinf* 8(4):289–302. <https://doi.org/10.1016/j.jag.2006.03.002>
- Bhuiyan C, Saha AK, Bandyopadhyay N, Kogan FN, Saha AK, Bandyopadhyay N, Analyzing FNK (2017) Analyzing the impact of thermal stress on vegetation health and agricultural drought—a case study from Gujarat, India. *Giosci Remote Sens* 00(00):1–22. <https://doi.org/10.1080/15481603.2017.1309737>
- Cai S, Zuo D, Xu Z, Han X, Gao X (2018) Spatiotemporal variability and assessment of drought in the Wei River basin of China. In: *Proceedings of the international association of hydrological sciences*, vol 379, pp 73–82. <https://doi.org/10.5194/piahs-379-73-2018>
- Choi M, Jacobs JM, Anderson MC, Bosch DD (2013) Evaluation of drought indices via remotely sensed data with hydrological variables. *J Hydrol* 476:265–273. <https://doi.org/10.1016/j.jhydrol.2012.10.042>
- Degefu MA, Bewket W (2015) Trends and spatial patterns of drought incidence in the omo-ghibe river basin, Ethiopia. *Geogr Ann Ser A Phys Geogr* 97(2):395–414. <https://doi.org/10.1111/geoa.12080>
- Dinku T, Ayeahu GT, Tadesse T, Gessesse B (2018) Validation of new satellite rainfall products over the Upper Blue Nile Basin, Ethiopia. *Atmos Meas Tech* 11(4):1921–1936. <https://doi.org/10.5194/amt-11-1921-2018>
- Edossa D, Babel M, Das Gupta A (2010) Drought analysis in the Awash River Basin, Ethiopia. *Water Resour Manag* 24(7):1441–1460. <https://doi.org/10.1007/s11269-009-9508-0>
- Evans JD (1996) *Straight forward statistics for the behavioral sciences*. Brooks/Cole, Pacific Grove
- Frey CM, Kuenzer C, Dech S (2012) Quantitative comparison of the operational NOAA-AVHRR LST product of DLR and the MODIS LST product V005. *Int J Remote Sens* 33(22):7165–7183. <https://doi.org/10.1080/01431161.2012.699693>
- Frey CM, Kuenzer C (2015) Analysing a 13 years MODIS land surface temperature time series in the Mekong Basin. In: Kuenzer C, Dech S, Wagner W (eds) *Remote sensing time series. Remote sensing and digital image processing*, vol 22. Springer, Cham. <https://doi.org/10.1007/978-3-319-15967-6>
- Gebrehiwot T, Van der Veen A, Maathuis B (2011) Spatial and temporal assessment of drought in the Northern highlands of Ethiopia. *Int J Appl Earth Obs Geoinf* 13(3):309–321. <https://doi.org/10.1016/j.jag.2010.12.002>
- Gebrehiwot T, Van der Veen A, Maathuis B (2016) Governing agricultural drought: monitoring using the vegetation condition index. *Ethiop J Environ Stud Manag* 9(3):354–371
- Gidey E, Dikinya O, Sebego R, Segosebe E, Zenebe A (2018) Analysis of the long-term agricultural drought onset, cessation, duration, frequency, severity and spatial extent using vegetation health index (VHI) in Raya and its environs, Northern Ethiopia. *Environ Syst Res*. <https://doi.org/10.1186/s40068-018-0115-z>
- Gu Y, Brown JF, Verdin JP, Wardlow B (2007) A five-year analysis of MODIS NDVI and NDWI for grassland drought assessment over the central Great Plains of the United States. *Geophys Res Lett* 34(6):1–6. <https://doi.org/10.1029/2006GL029127>
- Hassan S, Mahmud-ul-islam S (2015) Drought vulnerability assessment in the high barind tract of Bangladesh using MODIS NDVI and land surface temperature (LST) imageries. *Int J Sci Res* 4(2):55–60
- Haile BT, Bekitie KT, Zeleke TT, Ayal DY, Feyisa GL, Anose FA (2022) Drought analysis using standardized evapotranspiration and aridity index at bilate watershed: sub-basins of Ethiopian Rift Valley. *Sci World J*. <https://doi.org/10.1155/2022/1181198>
- Hayes M, Svoboda M, Wall N, Widhalm M (2011) The Lincoln declaration on drought indices: universal meteorological drought index recommended. *Bull Am Meteorol Soc* 92(4):485–488. <https://doi.org/10.1175/2010BAMS3103.1>
- Hurni H, Abate S, Bantider A, Debele B (2010) Land degradation and sustainable land management in the Highlands of Ethiopia. In: Hurni H, Wiesmann UM (eds) *Global Change and sustainable development: a synthesis of regional experiences from research*. Geographica Bernesia, Bern, Switzerland, vol 5, pp 187–207
- Ihinegbu C, Ogunwumi T (2021) Multi-criteria modeling of drought: a study of Brandenburg Federal. *Model Earth Syst Environ*. <https://doi.org/10.1007/s40808-021-01197-2>
- Jenkerson CB, Maiersperger T, Schmidt G (2010) eMODIS: a user-friendly data source. US Geological Survey. Open-File Report 2010–1055, 10 p
- Karnieli A, Bayasgalan M, Bayarjargal Y, Agam N, Khudulmur S, Tucker C (2006) Comments on the use of the vegetation health index over Mongolia. *Int J Remote Sens* 27(10):2017–2024. <https://doi.org/10.1080/01431160500121727>
- Karnieli A, Agam N, Pinker RT, Anderson M, Imhoff ML, Gutman GG, Panov N, Goldberg A (2010) Use of NDVI and land surface temperature for drought assessment: merits and limitations. *J Clim* 23(3):618–633. <https://doi.org/10.1175/2009JCLI2900.1>
- Katila M, Rajala T, Kangas A (2020) Assessing local trends in indicators of ecosystem services with a timeseries of forest resource maps. *Silva Fennica*, 54(4):1–19. <https://doi.org/10.14214/sf.10347>
- Kogan FN (1995) Application of vegetation index and brightness temperature for drought detection. *Adv Space Res* 15(11):91–100
- Kogan FN (2019) *Remote sensing for food security*. Springer International Publishing, Berlin
- Kogan FN, Guo W (2016) Early twenty-first-century droughts during the warmest climate. *Geomat Nat Hazards Risk* 7(1):127–137. <https://doi.org/10.1080/19475705.2013.878399>
- Kogan FN, Guo W, Yang W, Shannon H (2018) Space-based vegetation health for wheat yield modeling and prediction in Australia. *J Appl Remote Sens* 12(2):026002. <https://doi.org/10.1117/1.JRS.12.026002>
- Kogan FN, Guo W, Yang W (2019) Drought and food security prediction from NOAA new generation of operational satellites. *Geomat Nat Hazards Risk* 10(1):651–666. <https://doi.org/10.1080/19475705.2018.1541257>
- Li B, Zhang J, Yu Z, Liang Z, Chen L, Acharya K (2017) Climate change is driven water budget dynamics of a Tibetan inland lake. *Glob Planet Change* 150:70–80. <https://doi.org/10.1016/j.gloplacha.2017.02.003>
- Liou YA, Mulualem GM (2019) Spatiotemporal assessment of drought in Ethiopia and the impact of recent intense droughts. *Remote Sens* 11(15):1828. <https://doi.org/10.3390/rs11151828>
- Lu J, Carbone GJ, Gao P (2017) Agricultural and forest meteorology detrending crop yield data for spatial visualization of drought impacts in the United States, 1895–2014. *Agric for Meteorol* 237–238:196–208. <https://doi.org/10.1016/j.agrformet.2017.02.001>
- Ma’rufah U, Hidayat R, Prasasti I (2017) Analysis of relationship between meteorological and agricultural drought using standardized precipitation index and vegetation health index. *J Phys Conf Ser*. <https://doi.org/10.1088/1742-6596/755/1/011001>
- Mann HB (1945) Nonparametric tests against trend. *Econometrica*. <https://doi.org/10.2307/1907187>

- Miah MG, Abdullah HM, Jeong C (2017) Exploring standardized precipitation evapotranspiration index for drought assessment in Bangladesh. *Environ Monit Assess*. <https://doi.org/10.1007/s10661-017-6235-5>
- Mishra AK, Singh VP (2010) A review of drought concepts. *J Hydrol* 391(1–2):202–216
- Mishra D, Goswami S, Matin S, Sarup J (2022) Analyzing the extent of drought in the Rajasthan state of India using vegetation condition index and standardized precipitation index. *Modeling Earth Syst Environ* 8(1):601–610. <https://doi.org/10.1007/s40808-021-01102-x>
- Mohammed Y, Yimer F, Tadesse M, Tesfaye K (2018) Meteorological drought assessment in Northeast Highlands of Ethiopia. *Int J Clim Change Strateg Manag* 10:142–160. <https://doi.org/10.1108/IJCCSM-12-2016-0179>
- Mutsotso RB, Sichangi AW, Makokha GO (2018) Spatio-temporal drought characterization in Kenya from 1987 to 2016. *Adv Remote Sens* 7:125–143. <https://doi.org/10.4236/ars.2018.72009>
- Nam WH, Hayes MJ, Svoboda MD, Tadesse T, Wilhite DA (2015) Drought hazard assessment in the context of climate change for South Korea. *Agric Water Manag* 160:106–117. <https://doi.org/10.1016/j.agwat.2015.06.029>
- Neeti N, Eastman JR (2011) A contextual Mann–Kendall approach for the assessment of trend significance in image time series. *Trans GIS* 15:599–611. <https://doi.org/10.1111/j.1467-9671.2011.01280.x>
- Patil Abhijit S, Patil Akshay A, Patil Somnath P, Saundade Sushant D, Chugule Kusum A, Katavare Shital B, Panhalkar Sachin S (2021) Analysis of the agriculture drought severity and spatial extent using Vegetation Health Index (VHI) in Manganga watershed of Maharashtra, India
- Pérez-Hoyos A, Rembold F, Kerdiles H, Gallego J (2017) Comparison of global land cover datasets for cropland monitoring. *Remote Sens*. <https://doi.org/10.3390/rs9111118>
- Pohler T (2020) Trend: non-parametric trend tests and change-point detection. R package v.1.1.2. <https://cran.r-project.org/package=trend>
- Qian X, Liang L, Shen Q, Sun Q (2016) Drought trends based on the VCI and its correlation with climate factors in the agricultural areas of China from 1982 to 2010. *Environ Monit Assess*. <https://doi.org/10.1007/s10661-016-5657-9>
- Qu C, Hao X, Qu JJ (2019) Monitoring extreme agricultural drought over the Horn of Africa (HOA) using remote sensing measurements. *Remote Sens* 11(8):902
- Rahman MR, Lateh H (2016) Meteorological drought in Bangladesh: assessing, analyzing and hazard mapping using SPI, GIS, and monthly rainfall data. *Environ Earth Sci*. <https://doi.org/10.1007/s12665-016-5829-5>
- Sai MS, Murthy CS, Chandrasekar K, Jeyaseelan AT, Diwakar PG, Dadhwal VK (2016) Agricultural drought: assessment and monitoring. *Mausam* 67(1):131–142
- Segele ZT, Lamb PJ (2005) Characterization and variability of Kiremt rainy season over Ethiopia. *Meteorol Atmos Phys* 89(1):153–180. <https://doi.org/10.1007/s00703-005-0127-x>
- Sen PK (1968) Estimates of the regression coefficient based on Kendall's tau. *J Am Stat Assoc* 63(324):1379–1389
- Singh RP, Kogan FN, Oceanic N (2003) Vegetation and temperature condition indices from NOAA AVHRR data for drought monitoring over India. *Int J Remote Sens* 24(22):4393–4402. <https://doi.org/10.1080/0143116031000084323>
- Sohnesen TP (2020) Two sides to the same drought: measurement and impact of Ethiopia's 2015 historical drought. *Econ Disasters Clim Change* 4(1):83–101. <https://doi.org/10.1007/s41885-019-00048-w>
- Swets DL (1999) A weighted least-squares approach to temporal smoothing of NDVI. In: Proceedings of the 1999 ASPRS annual conference, from image to information, Portland. American society for photogrammetry and remote sensing, Bethesda, 17–21 May 1999
- Tadesse T, Sena GB, Berhan G, Regassa T (2015) Evaluating a satellite-based seasonal evapotranspiration product and identifying its relationship with other satellite-derived products and crop yield: a case study for Ethiopia. *Int J Appl Earth Obs Geoinf* 40:39–54. <https://doi.org/10.1016/j.jag.2015.03.006>
- Tucker CJ (1979) Red and photographic infrared linear combinations for monitoring vegetation. *Remote Sens Environ* 8(2):127–150. [https://doi.org/10.1016/0034-4257\(79\)90013-0](https://doi.org/10.1016/0034-4257(79)90013-0)
- Vicente-Serrano SM, Beguería S, López-Moreno JI (2010) A multiscalar drought index sensitive to global warming: the standardized precipitation evapotranspiration index. *J Clim* 23(7):1696–1718. <https://doi.org/10.1175/2009JCLI2909.1>
- Viste E, Korecha D, Sorteberg A (2013) Recent drought and precipitation tendencies in Ethiopia. *Theor Appl Climatol* 112(3):535–551. <https://doi.org/10.1007/s00704-012-0746-3>
- Wan Z (2006) MODIS land surface temperature products users' guide. Institute for Computational Earth System Science, University of California, Santa Barbara, p 805
- Wilhite DA (2011) Quantification of agricultural drought for effective drought mitigation and preparedness: key issues and challenges. In: Agricultural drought indices: Proceedings of the WMO/UNISDR expert group meeting, 2–4 June 2010, Murcia, Spain. World Meteorological Organization (WMO), Geneva, pp 13–21
- Wu Z, Huang NE, Long SR, Peng CK (2007) On the trend, detrending, and variability of nonlinear and nonstationary time series. *Proc Natl Acad Sci USA* 104(38):14889–14894
- Yisehak B, Zenebe A (2020) Modeling multivariate standardized drought index based on the drought information from precipitation and runoff: a case study of Hare watershed of Southern Ethiopian Rift Valley Basin. *Model Earth Syst Environ*. <https://doi.org/10.1007/s40808-020-00923-6>
- Zeng J, Zhang R, Qu Y, Bento VA, Zhou T, Lin Y, Wu X, Qi J, Shui W, Wang Q (2022) Improving the drought monitoring capability of VHI at the global scale via ensemble indices for various vegetation types from 2001 to 2018. *Weather Clim Extremes* 35:100412. <https://doi.org/10.1016/j.wace.2022.100412>

Publisher's Note Springer Nature remains neutral with regard to jurisdictional claims in published maps and institutional affiliations.